TD 98-058

Magnetic Field Measurements of HGQ003 – Test Summary Report V1.0

J. DiMarco, P. Schlabach

October 19, 1998

Contents

List of Figures

List of Tables

1 Introduction

This report presents preliminary results of measurements of the magnetic field of HGQ003 made at the FNAL Vertical Magnet Test Facility in August and September of 1998. HGQ003

is the third 70 mm-aperture, short model LHC quadrupole built at FNAL. We report only on magnetic measurements. Other aspects of the test program will be reported separately.

After a brief description of the measurement apparatus and program, we present relevant summaries of harmonics, comparisons to the first two magnets and other items of interest.

Magnetic measurements of HGQ003 were performed during two test cycles, most during the first. The first test cycle was conducted only at 4.5K. A malfunctioning valve prevented us from reaching 1.9K. Between test cycles, the VMTF dewar was warmed to room temperature to thaw out the valve. The magnet was not removed. The magnet was then tested at both 4.5K and 1.9K in the second test cycle.

2 Measurement Apparatus, Analysis

Magnetic measurements on HGQ002 were made and analyzed using the system described in [1], [2]. The probe has nominal diameter 4.1 cm and length 0.8 m

An additional length of driveshaft has been added to the measurement system allowing measurement in the non-lead end of the magnet. Measurement in the return end is now limited by the length of the warm bore, not the length of the drive shaft.

Field harmonics are computed at a reference radius of 17 mm. The measurement coordinate system is described in [3].

Further system, operations, and analysis information is available at

http://tsmtf.fnal.gov/~dimarco/sscl_systems.html.

3 Measurement Program

The list of measurements is given in Table 1. Measurements were concentrated on axial variation of field and current; time, and ramp rate dependence of harmonics. Additional measurements were done to compare warm measurements with 12 A magnet current to the nominal 10 A measurements (#5).

It should be noted that

1. Measurement #28 ended prematurely (on the 3rd of 3 up ramps at 10120 A).

Representative plots and summaries of harmonics from the main areas of measurement are given below. A complete set of plots for all measurements can be found at

http://tsmtf.fnal.gov/~dimarco/HGQ002_test_data.html

1	collared_coil	Axial scan of collared coil (10 A, warm, FE1 probe)
2	yoked_ib3_10A	Axial scan of cold mass (10 A, warm, FE1 probe)
3	bef_tc1_10A	Axial scan before test cycle 1 (10 A, warm, VMTF)
4	bef_tc1_12A	Axial scan before test cycle 1 (12 A, warm, VMTF)
5	r0800_8300Ah20_TCI_pos3	Loop to 8.3 kA, 20 A/s, 4.5 K, z=1.0 m pos., TCI
6	2kA_end_scan_TCI	Lead endscan at 2 kA, 4.5 K, TCI
7	2kA_zscan_TCI	Axial scan at 2 kA, 4.5 K, TCI
8	6kA_zscan_TCI	Axial scan at 6 kA, 4.5 K, TCI
9	8.3kA_end_scan_TCI	Lead endscan at 8.3 kA, 4.5 K, TCI
10	8.3kA_zscan_TCI	Axial scan at 8.3 kA, 4.5, TCI K
11	r0800_8300Ah20_TCI	Loop to 8.3 kA, 20 A/s, 4.5 K, TCI
12	Stair0_8300As1000w02_TCI	Stair-step loop to 8.3 kA, 4.5 K, TCI)
13	X1r08300Af05w00s30_TCI	Accelerator cycle with 5 min. 8.3 kA recycle current, 4.5 K, TCI
14	r0800_8300Ah80_TCI	Loop to 8.3 kA, 80 A/s, 4.5 K, TCI
15	r0800_8300Ah40_TCI	Loop to 8.3 kA, 40 A/s, 4.5 K, TCI
16	r0800_8300Ah20_TCI_pos2	Loop to 8.3 kA, 20 A/s, 4.5 K, z=0.706 m pos., TCI
17	r0800_8300Ah10_TCI	Loop to 8.3 kA, 10 A/s, 4.5 K, TCI
18	X1r08300Af15w00s30_TCI	Accelerator cycle with 15 min. 8.3 kA pre-cycle current 4.5 K, TCI
19	2kA_end_scan_TCII	Lead endscan at 2 kA, 1.9 K, TCII
20	2kA_zscan_TCII	Axial scan at 2 kA, 1.9 K, TCI
21	6kA_end_scan_TCII	Lead endscan at 6 kA, 1.9 K, TCII
22	6kA_zscan_TCII	Axial scan at 6 kA, 1.9 K, TCII
23	11kA_end_scan_TCII	Lead endscan at 11 kA, 1.9 K, TCII
24	11kA_zscan_TCII	Axial scan at 11 kA, 1.9 K, TCII
25	r0800_11000Ah20_TCII	Loop to 11 kA, 20 A/s, 1.9 K, TCII
26	X1r08300Af05w00s30_TCII	Accelerator cycle with 5 min. 11 kA recycle current, 1.9 K, TCII
27	r0800_11700Ah80_TCII	Loop to 11.7 kA, 80 A/s, 1.9 K, TCII
28	r0800_11000Ah10_TCII	Loop to 11 kA, 10 A/s, 1.9 K, TCII

Table 1: The following magnetic measurements have been performed on HGQ003. Except where noted, all measurements with fixed probe position were made at Z=0.819 m (near magnet center).

4 Transfer Function

Figure 1 shows the transfer function obtained from measurements 2kA_zscan and 6kA_zscan. Also plotted are field angle and the transverse plane probe offsets determined from the feed down of quadrupole to dipole. The magnet has some twist: 2-3 mrad/m.

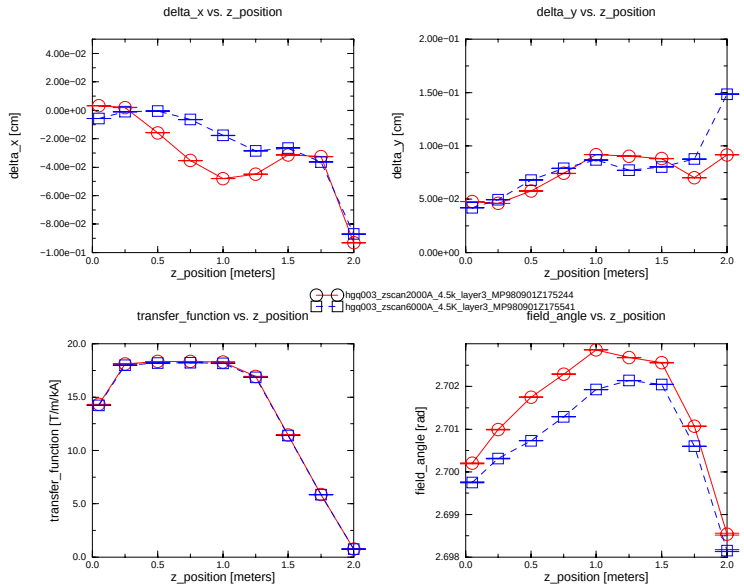

Figure 1: Transfer function, transverse probe offsets, field angle.

The measured transfer function of HGQ002 was 0.1-0.2% lower than that of HGQ001 [4]. At the time the HGQ002 test report was written, we had no explanation for this anomalous decrease. One possibility was that the calibrations of the different probes used for the two measurements were different. We have since found that during set up for use of the second probe we interchanged quad winding radii calibrations and that the reported transfer function for cold measurements of HGQ002 should be reduced 1.4%. [1] Thus the difference between the transfer functions in the first two magnets was much bigger (and even harder to explain). The HGQ003 transfer function is similar to that of HGQ002. We believe that approximately 1% of the difference in transfer functions between HGQ001 and HGQ002/3 is real. Examination of the warm measurements – all made by the 1 m mole probe – in IB3 show that HGQ002/3 gain 1% less strength when yoked than did HGQ001. The remaining difference in transfer function may be due to probe calibration. The VMTF probe was cross

[1] There is also a small change in harmonics. Reported harmonics should be multiplied by 1.02.

calibrated against an existing probe. We plan to check the calibration by comparing to our "MI standard" probe.

We have reported HGQ003 measurements using the same calibrations as were used in reporting HGQ002 measurements in spite of the fact that we know they are wrong. When we have a better understanding of the absolute calibration of the new VMTF probe, we will make the change.

5 Standard Harmonics

Tables 2, 3 and 4 summarize the field harmonics in the magnet body. Data are from measurement r0800_11000Ah20_TCII taken at $z = 0.819$ m.

02000 kA	(u)	(u)	(d)	(d)
n	mean	error	mean	error
b 3	1.007	0.01157	0.981	0.00286
b 4	0.182	0.00241	0.179	0.00154
b 5	-0.364	0.00138	-0.351	0.00103
b 6	-1.285	0.04690	-0.397	0.02350
b 7	-0.071	0.00052	-0.063	0.00041
b 8	-0.002	0.00046	-0.002	0.00028
b 9	0.001	0.00022	0.002	0.00020
b10	-0.040	0.00232	-0.061	0.00065
a 3	-0.463	0.01163	-0.437	0.00403
a 4	0.385	0.00441	0.364	0.00114
a 5	0.282	0.00153	0.259	0.00101
a 6	0.083	0.00227	0.060	0.00092
a 7	-0.034	0.00087	-0.026	0.00059
a 8	0.033	0.00040	0.031	0.00035
a 9	0.007	0.00033	0.007	0.00030
a10	-0.004	0.00015	-0.005	0.00028

Table 2: Field harmonics at 2 kA measured during the second test cycle. Separate values are given for the field during up ("u") and down ("d") ramp. (Data are averaged over the range ± 300 A around the nominal value The change in field with current over that range is small.) The quoted error is $\sigma/\sqrt{(N)}$, where N is the number of points included in the average.

6 Axial Scans

Figure 2 shows the variation in field along the magnet axis.

The smallest z position at which the probe could be positioned was 0.05 m due to the depth of the warm bore. In this position, the far end of the probe windings is approximately 0.2 m beyond the return end of the magnet, approximately 3 times the 70 mm magnet aperture. One would thus expect to capture nearly all of the magnet end field. At the lead

06000 kA	(u)	(u)	(d)	(d)
n	mean	error	mean	error
b 3	0.899	0.00164	0.899	0.00193
b 4	0.156	0.00050	0.160	0.00050
b 5	-0.371	0.00041	-0.367	0.00043
b 6	-1.050	0.00641	-0.840	0.00180
b 7	-0.068	0.00031	-0.065	0.00047
b 8	-0.004	0.00026	-0.003	0.00034
b 9	0.000	0.00026	0.000	0.00018
b10	-0.040	0.00034	-0.045	0.00021
a 3	-0.344	0.00241	-0.351	0.00121
a 4	0.378	0.00045	0.375	0.00069
a 5	0.286	0.00092	0.281	0.00057
a 6	0.082	0.00037	0.073	0.00035
a 7	-0.034	0.00043	-0.030	0.00040
a 8	0.032	0.00023	0.032	0.00018
a 9	0.008	0.00029	0.008	0.00016
a10	-0.005	0.00014	-0.005	0.00009

Table 3: Field harmonics at 6 kA measured during the second test cycle.

	02000	kA		06000	kA		11000	kA
n	mean	error	n	mean	error	n	mean	error
b 3	0.994	0.00648	b 3	0.899	0.00125	b 3	0.946	0.00068
b 4	0.180	0.00142	b 4	0.158	0.00053	b 4	0.162	0.00058
b 5	-0.357	0.00167	b 5	-0.369	0.00054	b 5	-0.385	0.00037
b 6	-0.841	0.10024	b 6	-0.941	0.02162	b 6	-1.001	0.00386
b 7	-0.067	0.00096	b 7	-0.067	0.00042	b 7	-0.066	0.00021
b 8	-0.002	0.00027	b 8	-0.003	0.00021	b 8	-0.003	0.00017
b 9	0.001	0.00019	b 9	0.000	0.00016	b 9	-0.001	0.00017
b10	-0.051	0.00255	b10	-0.043	0.00062	b10	-0.039	0.00013
a 3	-0.450	0.00664	a 3	-0.348	0.00151	a 3	-0.321	0.00094
a 4	0.375	0.00315	a 4	0.376	0.00054	a 4	0.401	0.00045
a 5	0.271	0.00271	a 5	0.284	0.00074	a 5	0.306	0.00043
a 6	0.071	0.00275	a 6	0.077	0.00086	a 6	0.084	0.00038
a 7	-0.030	0.00092	a 7	-0.032	0.00051	a 7	-0.031	0.00031
a 8	0.032	0.00034	a 8	0.032	0.00015	a 8	0.032	0.00021
a 9	0.007	0.00022	a 9	0.008	0.00016	a 9	0.009	0.00018
a10	-0.005	0.00019	a10	-0.005	0.00009	a10	-0.005	0.00009

Table 4: Field harmonics as measured during the second test cycle. Up and down ramp data have been averaged.

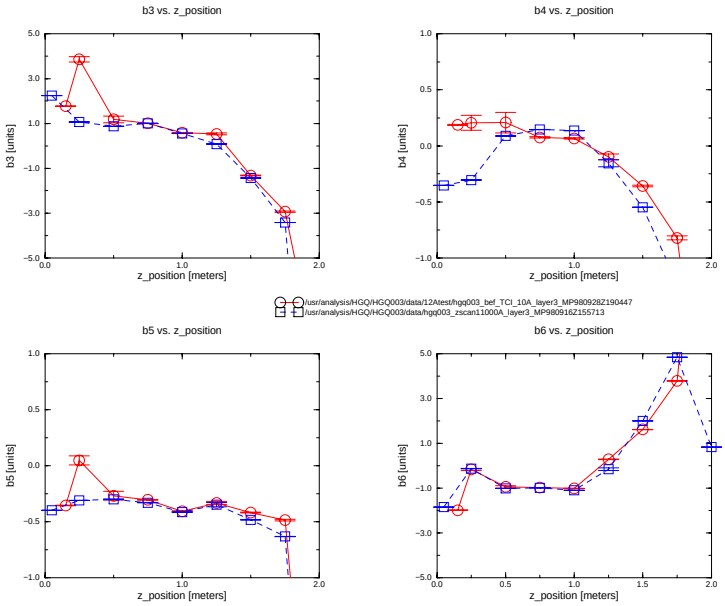

Figure 2: Warm and cold magnetic measurements vs. z. This is a representative plot comparing data from measurements bef_tc1_10A and 11kA_zscan_TCII.

end we expect that at a z position of about 1.9 m, the probe windings are entirely out of the body of the magnet.

7 Scan of Magnet Lead End

Fig. 3 shows the transfer function and the field angle obtained from measurement 11kA_end_scan_TCII.

As a figure of merit we characterize the end field by the harmonics at z=2.0 m normalized to the body field (z=1.0 m).[2] End field harmonics are given in Table 5 for HGQ002 (11kA_end_scan) and HGQ003 (11kA_end_scan_TCII).[3] One can see that the normal dodecapole is much smaller while the sextupole has increased somewhat.

[2] At the 2 m position, the probe should see only end field where we define the end region as beginning at the transition from normal to full round collars.

[3] Since the end field is truly 3 dimensional, we can't compare to measurements of HGQ001 which were made with a smaller radius probe.

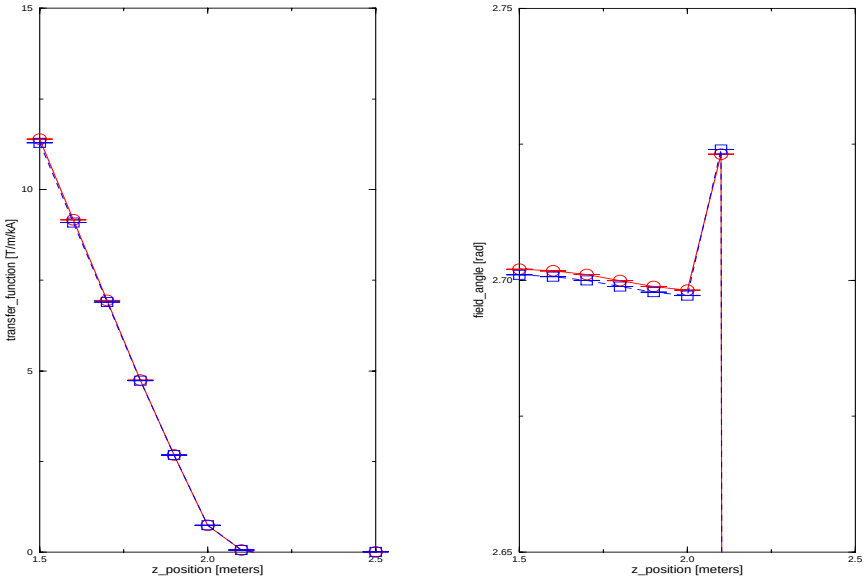

Figure 3: Transfer function and field angle as function of z in the lead end.

	ratio of TF		n= 3	4	5	6	7	8	9	10
HGQ002	0.15	b_n	0.23	0.21	0.20	2.48	0.02	-0.02	0.00	-0.08
		a_n	0.35	-0.33	-0.15	-0.12	-0.01	-0.01	0.01	-0.00
HGQ003	0.04	b_n	-0.78	-0.23	-0.18	0.04	-0.02	-0.01	0.00	-0.02
		a_n	-0.46	-0.23	0.01	0.24	-0.02	-0.01	-0.01	0.01

Table 5: End field harmonics in HGQ002 and HGQ003 normalized to the body field strength. The ratio of field strength in the end to that in the body is also given.

8 Variation of Hysteresis with Cycle Number

As was observed for HGQ002 but not for HGQ001, b_6 hysteresis during the first up ramp differs from that of other cycles. Measured dodecapole for 3 cycle loops from 800 to 11000 kA at 10 and 80 A/s ramp rate is plotted in Fig. 4. One can clearly see that the first cycle up ramp follows a different path from the second and third. These cycles, as are all such measurements, were preceeded by a cleansing quench. It is, perhaps, not so surprising that the first cycle following a cleansing quench is different. What is interesting, however, is that this behaviour was not seen in HGQ001.

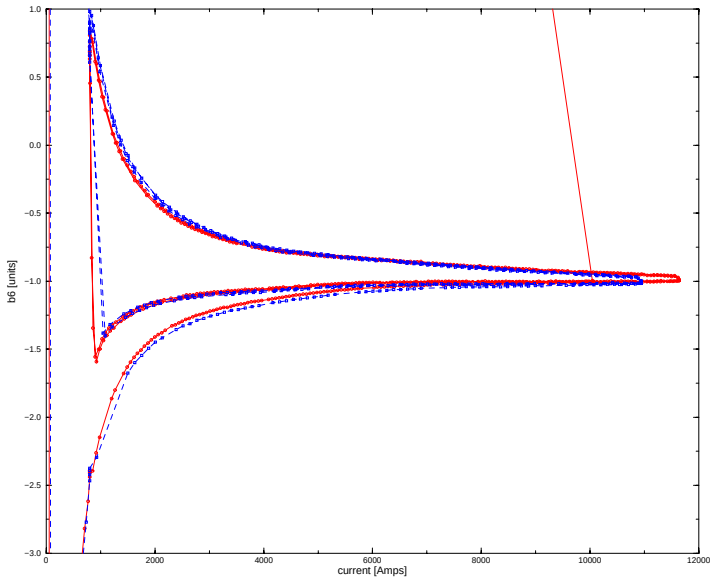

Figure 4: Measured b_6 during hysteresis loops. Data is taken from measurements r0800_11700Ah10_TCII and r0800_11700Ah80_TCII.

9 Variation of Hysteresis with Axial Position

As was reported for HGQ002, field hysteresis varies with axial position. The width of the hysteresis loop at 0.706 and 0.819 m position is the same. A large increase (> 0.25 units for sextupole, octupole, and decapole) is seen in the measurement made at 1 m.

10 Time Dependent Effects

Time dependent effects are observed in the field angle measured during hysteresis loops and at injection current during accelerator cycles.

10.1 Field angle to 11 kA

As was reported for the first two magnets, a clear ramp rate dependence of the skew quadrupole is observed as hysteresis in field angle with magnitude of the hysteresis half-width at 2000A being about 1mrad/10A/s[4] (1 mrad corresponds to 20 units of skew quadrupole).

10.2 Accelerator cycle ramps

Table 6 gives the change in field from the beginning to the end of a 30 min. injection plateau for measurements of HGQ002 (X1r0900Af05w00s30) and HGQ003 (X1r08300Af05w00s30_TCII). The behavior is much the same in the two magnets. The largest change is 0.7-0.8 units in b_6.

	HGQ002		HGQ003	
n	Δb_n	Δa_n	Δb_n	Δa_n
3	0.01 ± 0.03	0.04 ± 0.03	0.09 ± 0.02	-0.05 ± 0.02
4	0.02 ± 0.01	-0.01 ± 0.01	0.01 ± 0.01	-0.06 ± 0.01
5	0.00 ± 0.01	-0.02 ± 0.01	-0.05 ± 0.01	0.03 ± 0.01
6	-0.80 ± 0.00	-0.01 ± 0.01	-0.73 ± 0.01	0.00 ± 0.01
7	-0.01 ± 0.00	0.01 ± 0.00	0.00 ± 0.00	0.00 ± 0.00
8	0.00 ± 0.00	0.00 ± 0.00	0.00 ± 0.00	0.00 ± 0.00
9	0.00 ± 0.00	0.00 ± 0.00	0.00 ± 0.00	0.00 ± 0.00
10	-0.01 ± 0.00	0.00 ± 0.00	-0.01 ± 0.01	0.00 ± 0.00

Table 6: Change in field during a 30 min. injection plateau.

11 Distortion of Magnetic Field During Ramping

A reproducible change in the sextupole field during ramping of the magnet was seen during testing of HGQ002 [2]. The field change was correlated with the capture of so-called snapshot events [6]. Similar field distortions (Fig. 5) of the same magnitude (0.1 unit) are seen in the data from HGQ003 and occur at approximately the same currents during up and down ramp as the field changes seen in HGQ002. As was true during testing of HGQ002, the field changes and snapshot events are seen at the same current ranges. There is less snapshot

[4] 1.4, 0.8, 0.7 mrad/10A/s for HGQ001, 2, 3, respectively.

data during testing of HGQ003 since more of the testing took place at 4.5K where the events are rare.

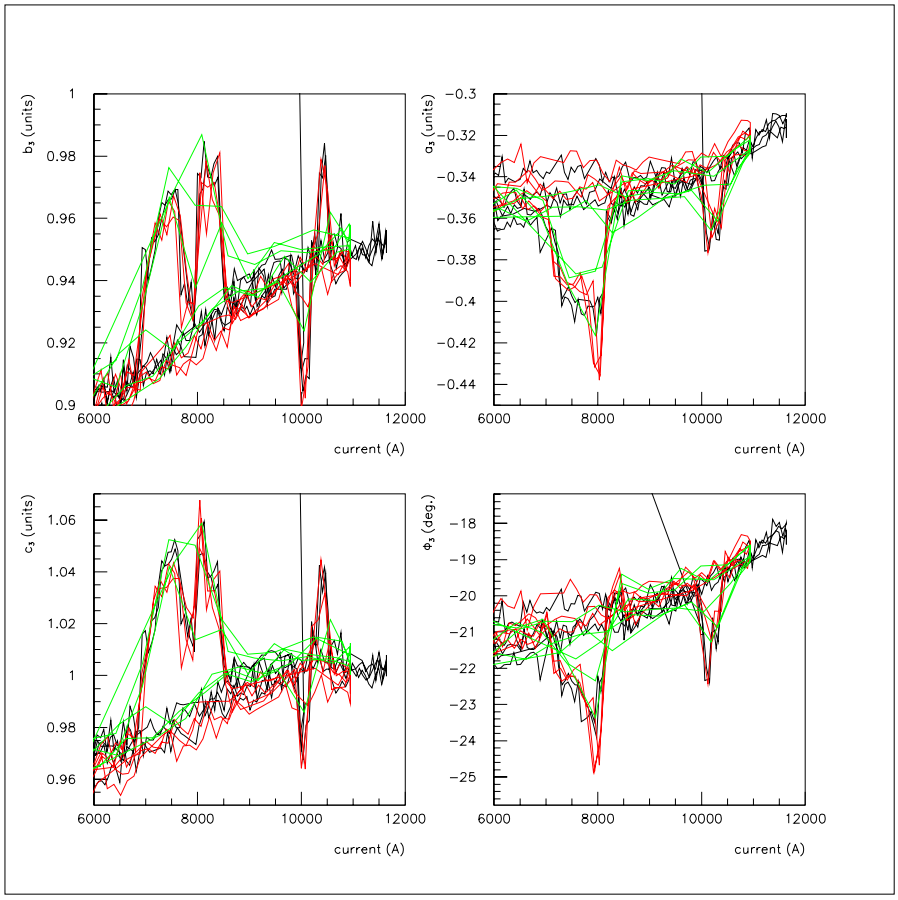

Figure 5: Sextupole field during 10 (r0800_11000Ah10_TCII), 20 (r0800_11000Ah20_TCII), 80 A/s (r0800_11700Ah80_TCII) hysteresis loop cycles. A field distortion is seen between 10000 and 10500 A on the up ramp and between 7000 and 8000 A on the down ramp.

12 Performance of the Measurement System

We comment on various aspects of the system performance.

12.1 Drive System

The section of drive shaft inserted to get into the magnet return end has significant bow. The extra section also increases the total unsupported length of drive shaft, particularly when measuring at lead end of the magnet. The bow causes significant distortions of the shaft, which increase as the unsupported length of shaft increases. Although the probe is supported in the warm finger at both ends and decoupled from the drive shaft sections by several flexible couplings, it was our impression that warm measurements were somewhat degraded due to the extra drive section. One could see changes in the raw voltage signals from position to position during the warm axial scans that may be due to probe/shaft vibration. A quantitative analysis needs to be done to determine if there are significant changes in the motion as a function of position.

12.2 Comparison of Warm Measurements at 10 and 12 A

Warm measurements are made at 10 A. To investigate whether signal size is a limiting factor in warm measurements, a measurement was taken at one axial position at 12 A – the maximum current the power supply can deliver. Comparison of the standard warm axial scan at 10 A (bef_tc1_10A) and the measurement with a current of 12 A (bef_tc1_12A) is shown in Fig. 6-9. The 12 A measurement is significantly improved compared to the 10 A measurement at the same axial position. The uncertainty is smaller. In addition, one can see that the measurement is much more consistent with the adjacent points. The uncertainty is, however, comparable to measurements made at 10 A at some of the other points (e.g. 1.0 m). Although the measurement at 12 A at this axial position is clearly better, it isn't obvious that this is due to the 20% increase in current. We may have simply chosen a fortuitous point for the comparison.

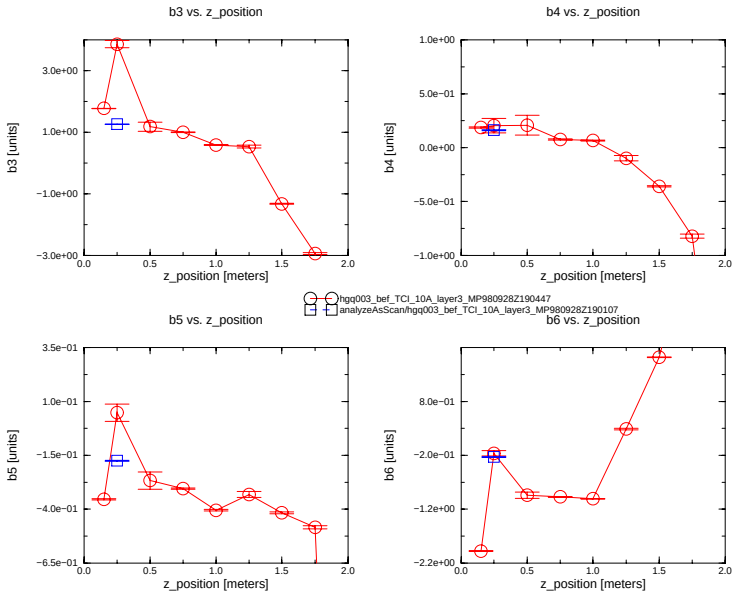

Figure 6: Comparison of the low order normal harmonics measured warm with 10 and 12 A magnet current. (The 12 A measurement is wrongly labled "10 A" on the plot.)

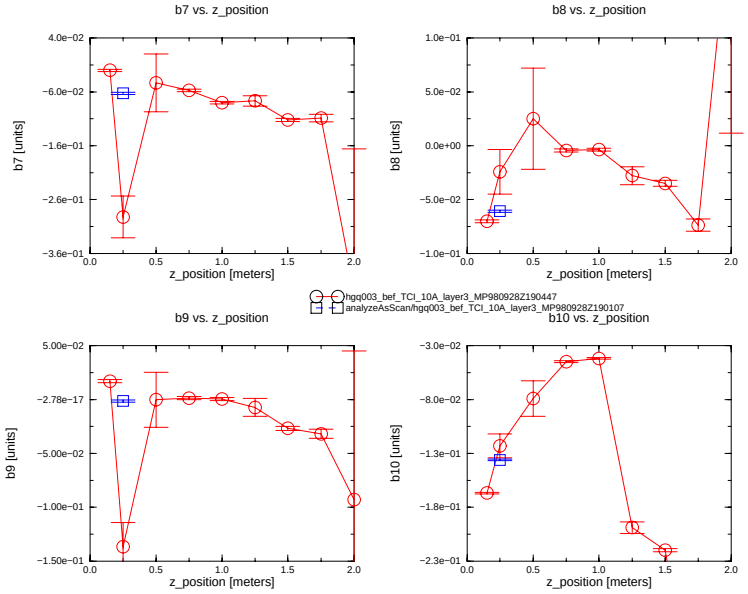

Figure 7: Comparison of the high order normal harmonics measured warm with 10 and 12 A magnet current.

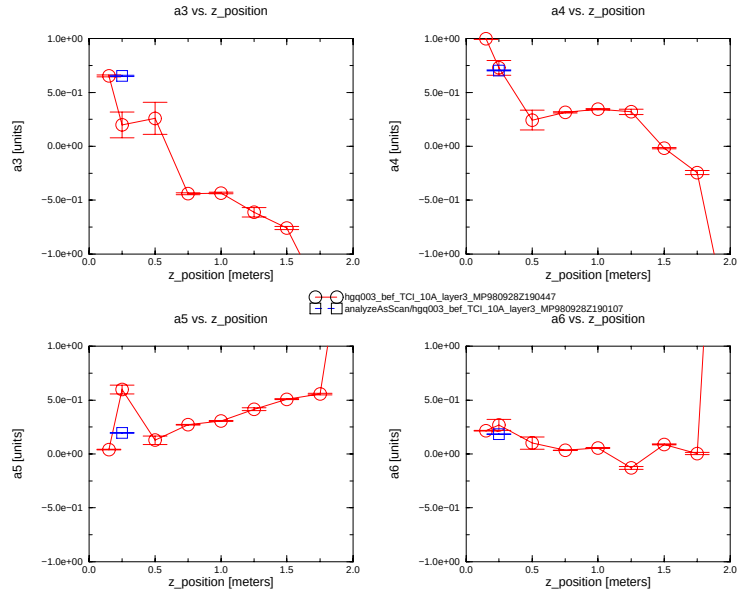

Figure 8: Comparison of the low order skew harmonics measured warm with 10 and 12 A magnet current.

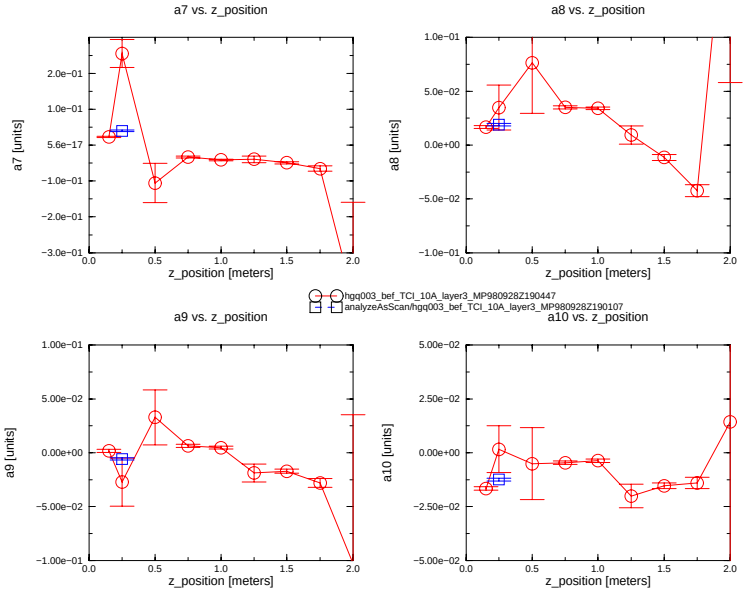

Figure 9: Comparison of the high order skew harmonics measured warm with 10 and 12 A magnet current.

12.3 Measurement Uncertainty

The measurement system has evolved during tests of the first 3 short model magnets. HGQ001 was measured with a 0.013 m radius, 0.3 m length probe while HGQ002 and HGQ003 were measured with a 0.020 m radius, 0.8 m length probe. The later probe produces a much larger signal, particularly for higher order field harmonics ($\Phi \approx R^n$). At the same time probe support and drive mechanics were improved. From the point-to-point variation in the field during a hysteresis loop shown in Fig. 10, we can see that the system performance was considerably improved during measurements of the last two magnets compared to the first. We quantify this by examining the variation in the field at constant current. To remove effects off field drift, we look at a relatively short period of time and fit the field as a function of time to a line. We then look at the residuals relative to that line (Fig. 11). The spread in the residuals is a factor of 40 or so smaller with the new probe and drive mechanics. It is similar for HGQ002 and HGQ003.[5]

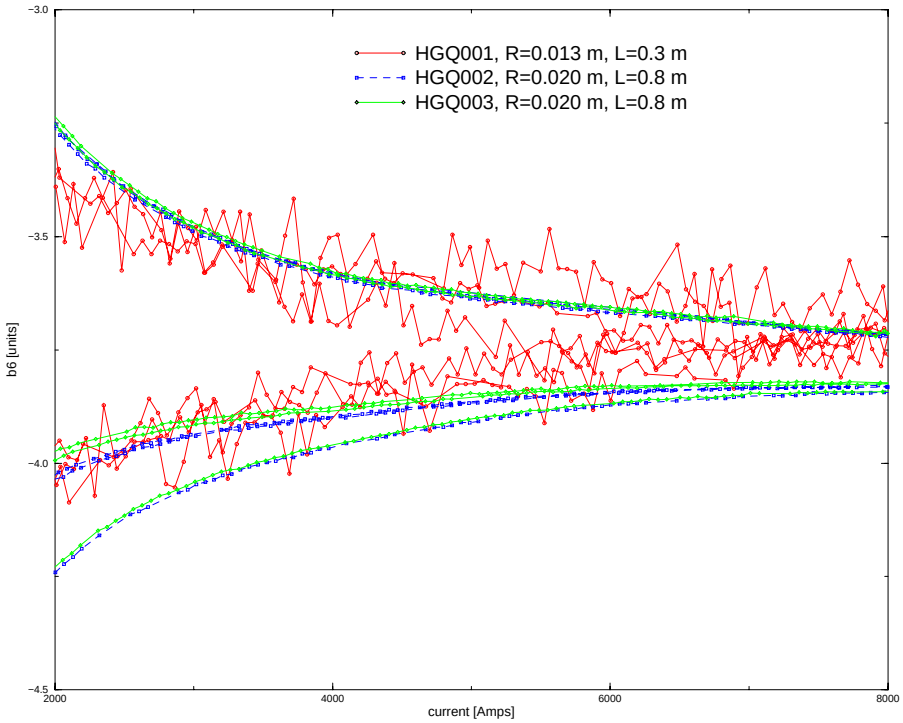

Figure 10: Measurement variation during a hysteresis loop. Overlaid are measurements of b_6 in the 3 magnets measured so far (arbitrary b_6 offset added).

[5] We had an additional 1 m length of drive shaft for measurement of HGQ003. This does not seem to have worsened system performance.

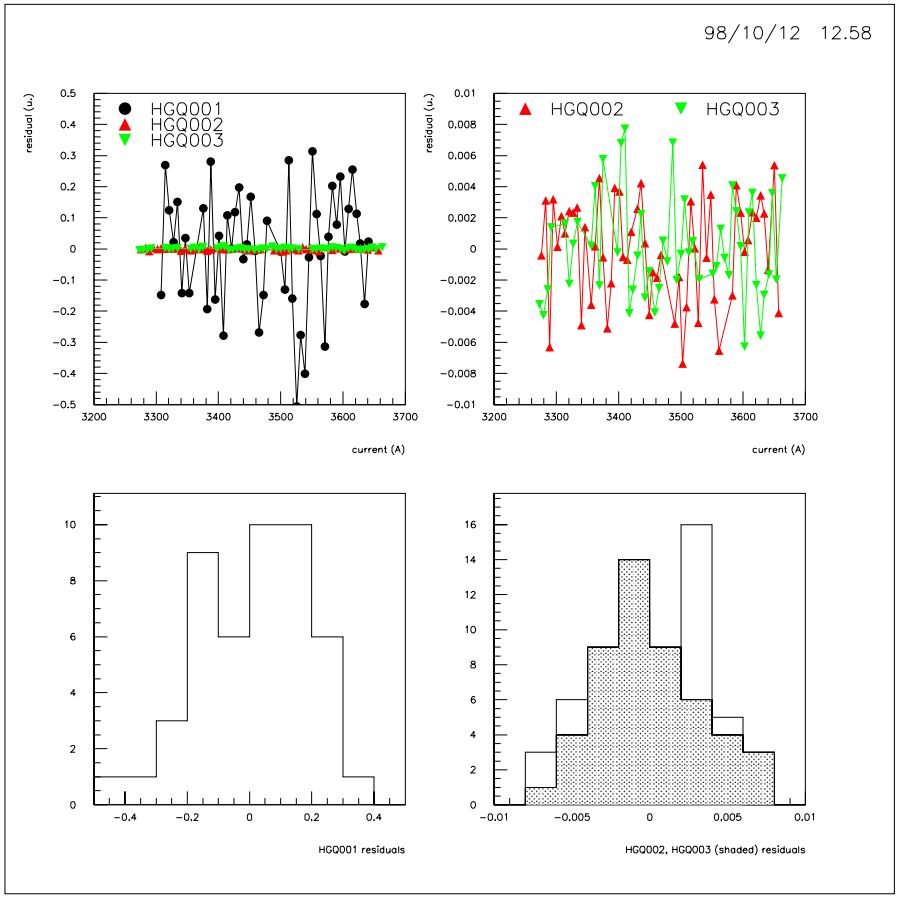

Figure 11: Measurement variation at injection current. At top are overlaid residual b_6 after subtracting from a linear fit to the field. On the left are shown residuals for the 3 magnets; and, on the right on an expanded scale, residuals for HGQ002 and HGQ003. At bottom left is a plot of the residuals for measurements of HGQ001; and, on the right, the residuals for measurements of HGQ002 and HGQ003.

13 Summary

We make the following observations about the magnet.

1. Axial variation is observed at a level greater than 2 units in most low order multipoles (b_3-b_6, a_3, a_4, a_6).

2. Normal and skew harmonics for $n \geq 8$ are less than 0.04 units in the body of the magnet. Table 7 summarizes field quality in the first 3 short models [5]. The field has

n	Normal (b_n)			Skew (a_n)		
HGQ	01	02	03	01	02	03
3	0.36	-0.70	1.04	0.27	0.55	-0.30
4	0.26	0.18	0.14	2.00	0.53	0.32
5	-0.29	0.09	-0.34	0.02	-0.17	0.26
6	-3.91	-1.54	-1.02	-0.08	0.03	0.07
7	-0.08	-0.01	-0.06	-0.05	0.00	-0.03
8	0.06	0.01	0.00	0.02	0.02	0.03
9	0.04	0.00	0.00	0.01	-0.01	0.01
10	-0.10	-0.10	-0.04	0.02	0.00	-0.01

Table 7: Field harmonics measured at magnet center at 6 kA.

   consistently improved as magnet manufacturing procedures have improved.

3. Harmonics show little change as a function of current. The biggest variation is 0.2 units in b_6 (identical to HGQ002).

4. Time dependent behavior is similar to that exhibited by HGQ002.

5. There is a measurable twist in the magnet.

6. The field during the first cycle of a hysteresis loop is different from the second and third.

7. The width of the hysteresis loop varies with axial position.

8. The sextupole field distortion seen during ramping is 0.1 units as it was in HGQ002. No attempt was made to localize the distortion along the length of the magnet.

References

[1] J. DiMarco, *et. al.*, "HGQS01 Test Summary Report", TD-98-025, (1998)

[2] J. DiMarco, P. Schlabach, "Magnetic Field Measurements of HGQ002 – Test Summary Report", TD-98-045, (1998)

[3] J. DiMarco, M. Lamm, G. Sabbi, P. Schlabach, "Conventions for HGQ Field Quality Representation",TD-98-036 , (1998)

[4] R. Bossert, *et. al.*, "Analysis of Magnetic Measurements of Short Model Quadrupoles for the LHC Low-β Insertions", Proc. EPAC Conf., (1998)

[5] R. Bossert, *et. al.*, "Magnetic Measurements of the Fermilab High Gradient Quadrupoles for the LHC Interaction Regions", Proc. ASC98 Conf., (1998)

[6] P. Schlabach, "Analysis of Sextupole Field Distortions and "Snapshot" Events During Testing of HGQ001 and HGQ002", TD-98-056, (1998)